Estimation of Correlation between Texture Features and Surface Parameters for Milled Metal Parts

Konstantin Trambitckii, Katharina Anding, Lilli Haar and Gunther Notni
Institute of Mechanical Engineering, Department of Quality Assurance and Industrial Image Processing, Ilmenau University of Technology, Gustav-Kirchhoff-Platz 2, Ilmenau, Germany

Keywords: Quality Assurance, Image Processing, Texture Features, Roughness Parameters, Metal Parts.

Abstract: Fast developing of computer technologies led to vast improvements of image processing systems and algorithms. Nowadays these algorithms are widely used in different areas of computer and machine vision systems. In this research texture features were used to analyse metal surfaces using a set of images obtained with industrial camera with macro lens. This kind of contactless surface roughness estimation is cheaper and quicker in comparison with traditional methods. A set of 27 texture features were calculated for a set of surface images. Correlation coefficients between the texture features and 10 roughness parameters for the sample surfaces were estimated. Obtained results showed that texture features can be successfully used for quick surface quality estimation.

1 INTRODUCTION

Quality assessment of machined surfaces is an important step in quality control of the industrial production process. It is used to check whether current quality of a surface fulfil given requirements. There are two groups of quality assessment methods: contact and contactless. Contact measurements with a profilometer is a traditional way of surface roughness control. The main disadvantages of contact methods are slow speed of quality assessment and physical damage of the measured surface caused by a probe of the measurement device. Another modern alternative is a group of contactless methods, where surface roughness can be estimated without any physical contact between a measuring device and a surface.

Nowadays great progress can be observed in the field of computer technologies. Its development led to vast improvement of image processing systems and algorithms. These algorithms are widely used in different areas of computer or machine vision systems.

2 STATE OF THE ART

Texture features are successfully used in various fields of image processing. Authors of different papers proposed various methods of optical surface quality control with help of texture features.

Figure 1: A sample of a metal part.

Some lenses of industrial cameras have small working distances. It can lead to a narrow depth of field on the resulting image. If a surface has a complex shape, which has large deviations from a focal plane of the camera, some parts of the surface can be not in-focus. This results in images having regions with less information in comparison with regions which are in-focus. In paper (Trambitckii et al., 2014) authors used in their research a set of texture features to segment such out-of-focus regions in the images of metal surfaces. Thus, only the segmented in-focus regions can be used in further steps. Haralick et al. (Haralick et al., 1973) described features, which

Trambitckii, K., Anding, K., Haar, L. and Notni, G.
Estimation of Correlation between Texture Features and Surface Parameters for Milled Metal Parts.
DOI: 10.5220/0007344104210428
In *Proceedings of the 8th International Conference on Pattern Recognition Applications and Methods (ICPRAM 2019)*, pages 421-428
ISBN: 978-989-758-351-3

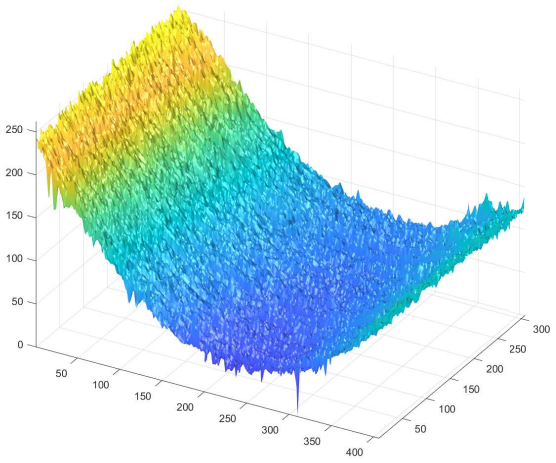

Figure 2: Samples of the surface scan of region №11 of part №10.

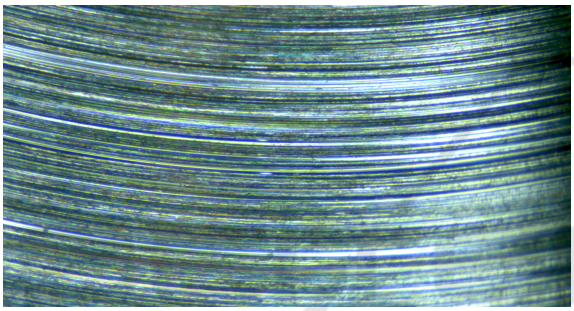

Figure 3: Samples of the photo of region №16 of part №7.

are calculated from grey level co-occurrence matrix (GLCM). This matrix can be calculated in various directions and different distances relative to neighbourhood pixels. Then a set of features can be estimated for a set of several GLMCs. These features describe different statistical information of an image and they are successfully used in the field of surface quality control (Alegre et al., 2010) and other fields of image processing (Chandraratne et al., 2006; Sabino et al., 2004; Torabi et al., 2007). The biggest weakness of the GLMC is that it has high computational complexity.

Li Liu et al. (Liu et al., 2012) used generalized local binary patterns (LBP) for texture classification. Difference-based and intensity-based features were extracted from local patches. Then they were combined into joint histograms. The classification based on these histograms showed good results on the challenging texture datasets.

A review of methods for prediction of surface quality was made by several authors (Benardos and Vosniakos, 2003; Lu, 2008). Texture features can be successfully applied for prediction of surface quality. Chen et al. (Chen et al., 2008) described a method of

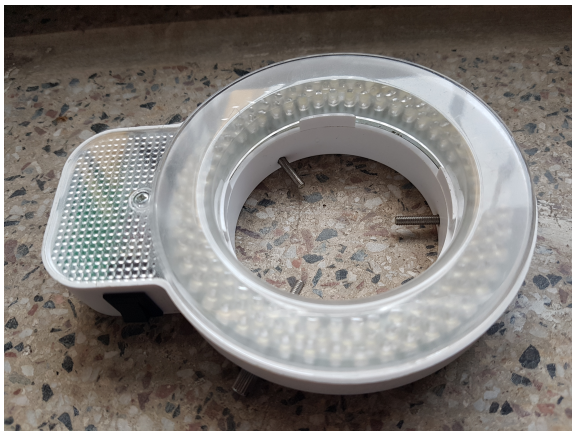

Figure 4: Ring light source used in the research.

estimation of the surface roughness using grey level co-occurrence matrix under the conditions of ambient light. Authors noticed that the ambient light affects calculated features. A new multivariate-based method was used to minimize the influence of the ambient light. Furthermore, it is important to consider the light direction and the quality of the light used to obtain the surface images. In the previous researches (Trambitckii et al., 2016) the correlation between texture features and roughness parameters was estimated. Results of the research showed that ring light can be a reliable light source for the tasks of surface quality assessment using an industrial camera. The main advantage of the ring light is its rotational invariance.

In this research, a set of focus texture features (listed in Chapter 4.2) is used to analyse the surface quality of metal parts under the conditions of a ring light source. The focus texture features were selected for this research because such features can reflect and deliver the information about a surface shape under appropriate lighting conditions. Correlation coefficients between the texture features and a set of roughness parameters (listed in Chapter 4.3), calculated for the sample surfaces, is estimated. In contrast with the previous researches (Trambitckii et al., 2016), where the correlation was estimated for the same areas of metal parts, in this paper the comparison of features and parameters will be performed for different areas of metal parts. Results of this research help to understand, how the set of texture features can be used for quick surface quality assessment.

3 DATA ACQUISITION

In this research, metal parts with cone-shaped surfaces were used (see Figure 1). The region of interest

has the size around 1 mm × 1 mm. 3D surface roughness was obtained with the Alicona 3D Infinite Focus G4 measurement system. A lens with the magnification of 20X was used. The lateral resolution (along X- and Y-axis) of the measurement system with 20X lens is 2.93 μm, the vertical resolution (along the Z-axis) is around 100 nm. The sample of surface image is shown in Figure 2.

2D images were obtained with a 2.23 MPix industrial camera IDS UI-3360CP-C-HQ with an attached telecentric macro lens. The camera has a resolution of 2048 px × 1088 px and the physical size of the sensor is 2/3". The macro lens attached to the camera has a changeable magnification rate of 0.8X-4X. It gave a possibility to make the region of interest similar to the one obtained with 3D Alicona system. The aperture of the lens cannot be stopped all the way down, because of the strong decrease of sharpness caused by diffraction. So the aperture was stopped about halfway down to get the sharpest possible images and a wider depth of field.

As was mentioned in the introduction, in optical measurements of metal surfaces light plays an important role because of the complex reflectance characteristics of such surfaces. In this research, the ring light source was used. The advantage of the ring light is its rotation invariance of shadows of surface images relative to the lighting source. A sample image of the surface obtained with a 2D camera is shown in Figure 3. The ring light source used in this paper is presented in Figure 4. The observed workpiece area of the metal surface is a countersink. The cutting speed of the tool, used to produce these drill hole, varied from 175 to 185 m/min, to get a different level of roughness. Thirteen metal parts were processed such a way. For each part, it was taken about twenty 2D images. It was measured the same amount of 3D data for the same set of metal parts. This resulted in 250 2D images and 250 3D surfaces.

4 ESTIMATION OF CORRELATION

4.1 Data Processing

For calculation of features and parameters, each image and surface was cropped. Cropping removes areas of images near the edges. The edges are less sharp than the centre areas. Also, Alicona 3D system and IDS industrial camera have different aspect ratios. After cropping 2D images and 3D surfaces both have the same aspect ratio, which is necessary for the next calculations.

Table 1: Amount of data for correlation estimation.

	2D Images	3D Surfaces
Amount	250	250
Features/Parameters	27	10

In the next step, every image and surface is divided into a grid of several subregions. Each feature and parameter was calculated for every of such subregions. The sizes of subregions were picked in such a way that both output matrices had the same size. This resulted in two equal-dimension sets of matrices: 2D texture features and 3D roughness parameters. Then the values of each matrix were averaged. These calculations resulted in a set of 27×250 mean values of texture features and 10×250 mean values of roughness parameters. These values are presented in Table 1.

4.2 Texture Features

27 different texture features were calculated in MATLAB environment for a set of surface images, obtained with the industrial camera. In this chapter, texture features which were used in this research are described.

4.2.1 Histogram Entropy

(F_{HEN}). It is a statistical feature of randomness that can be used to characterize the texture of an image. It is calculated by (C. Gonzalez et al., 2004; Firestone et al., 1991):

$$F_{HEN} = -\sum_{k}(p_k \log_b(p_k)) \,, \tag{1}$$

where k is the number of grey levels, $b = 2$ is the base of the log function to express entropy in bits, and p_k is the probability that the grey level k occurs in image:

$$p_k = \frac{h(k)}{D}, \tag{2}$$

where D is the number of pixels in the image.

4.2.2 Histogram Range

(F_{HRA}). It is the difference between maximum grey level and minimum grey level of an image (Firestone et al., 1991):

$$F_{HRA} = max\,(k|h(k) > 0) - min\,(k|h(k) > 0) \,, \tag{3}$$

where $h(k)$ is the value of the histogram h for the k-th grey level.

4.2.3 Image Curvature

The grey level intensity of pixel (x,x) will be denoted as $g(x,y)$. If the grey levels are treated as a 3D surface $(x,y,g(x,y))$, the curvature in a sharp image area is expected to be higher than in an unsharp area (Helmli and Scherer, 2001). The first step in calculating a feature, based on curvature, is to approximate the surface $f(x,y) = p_0x + p_1y + p_2x^2 + p_3y^2$. The coefficients $P = (p_0, p_1, p_2, p_3)^t$ are found using a least squares approximation (Nayar et al., 1996) with g_0 and g_2:

$$g_0 = \begin{pmatrix} -1 & 0 & 1 \\ -1 & 0 & 1 \\ -1 & 0 & 1 \end{pmatrix}, \quad (4)$$

$$g_2 = \begin{pmatrix} 1 & 0 & 1 \\ 1 & 0 & 1 \\ 1 & 0 & 1 \end{pmatrix}, \quad (5)$$

$$P = (\frac{g_0 * I}{6}; \frac{g_0^t * I}{6}; \frac{3g_2 * I}{10} - \frac{g_2^t * I}{5}; -\frac{g_2 * I}{5} + \frac{g_2^t * I}{10})^t . \quad (6)$$

Then these coefficients are combined in order to form a texture feature. An experimental evaluation (Helmli and Scherer, 2001) shows that the simple sum of the absolute values results in an adequate focus measure F_{ICU}:

$$F_{ICU} = |p_0| + |p_1| + |p_2| + |p_3| . \quad (7)$$

4.2.4 Steerable Filter-based

A focus texture feature F_{STEF} is based on steerable filters. Steerable filters represent a way to synthesize filters of arbitrary orientation using a linear combination of basis filters. Such synthesis is used to determine analytically the filter output as a function of orientation (Minhas et al., 2009b).

4.2.5 Spatial Frequency

Let denote the number of horizontal and vertical pixels of the image as M and N, respectively. Frequencies for rows and columns are defined by (M. Eskicioglu and S. Fisher, 1996):

$$RFreq = \sqrt{\frac{1}{M \cdot N} \sum_{x=1}^{M} \sum_{y=1}^{N} |g(x+1,y) - g(x,y)|^2} \quad (8)$$

and

$$CFreq = \sqrt{\frac{1}{M \cdot N} \sum_{x=1}^{M} \sum_{y=1}^{N} |g(x,y+1) - g(x,y)|^2} . \quad (9)$$

Thus, spatial frequency F_{SFR} is defined as

$$F_{SFR} = \sqrt{(RFreq)^2 + (CFreq)^2} . \quad (10)$$

4.2.6 Other Texture Features

Along with the listed texture features, also following features were tested on the samples surfaces: absolute central moment (Shirvaikar, 2004), Brenner's focus measure (Santos et al., 1997), image contrast (Nanda and Cutler, 2001), image curvature (Helmli and Scherer, 2001), DCT (discrete cosine transform) energy (Shen and Chen, 2006), DCT energy ratio (Lee et al., 2009), Gaussian derivative (Geusebroek et al., 2000), variance of grey-level (Krotkov and Martin, 1986), local variance of grey-level (Pech-Pacheco et al., 2000), normalized variance of grey-level (Santos et al., 1997), energy of gradient (Subbarao et al., 1992), thresholded gradient (Santos et al., 1997), squared gradient (M. Eskicioglu and S. Fisher, 1996), Helmli's measure (Helmli and Scherer, 2001), histogram entropy (Krotkov and Martin, 1986) and histogram range (Firestone et al., 1991), energy of Laplacian (Subbarao et al., 1992), modified Laplacian (Nayar et al., 1996), variance of Laplacian (Pech-Pacheco et al., 2000), diagonal Laplacian (Thelen et al., 2009), steerable filters-based (Minhas et al., 2009a), spatial frequency (M. Eskicioglu and S. Fisher, 1996), Tenengrad (Krotkov and Martin, 1986), Tenengrad variance (Pech-Pacheco et al., 2000), Vollat's correlation-based (Santos et al., 1997), wavelet sum (Yang and Nelson, 2003) and wavelet variance (Yang and Nelson, 2003).

4.3 Roughness Parameters

The surface quality can be estimated using roughness parameters established in international standards (ISO 25178). In this research the following ISO roughness parameters were used: S_a (arithmetical mean deviation of the assessed surface), S_q (root mean square deviation of the surface), S_{sk} (skewness of the surface), S_{ku} (kurtosis of the surface), S_v (maximum valley height of the surface), S_p (maximum peak height of the surface), S_z (maximum height of the surface, i.e. the difference between the highest peak and the deepest valley), S_{dq} (root mean square surface slope) and S_{dr} (developed interfacial area ratio). Along with the ISO parameters listed above another roughness parameter from other source was used - S_{sc} (mean summit curvature) (Stout et al., 1994).

Figure 5: Correlation coefficient distribution between different pairs of texture features and roughness parameters.

4.4 Evaluation of Correlation

Having two variable sets of the same size, Pearson's correlation coefficient can be estimated between them:

$$\rho(a,b) = \frac{\sum(a-\bar{a})(b-\bar{b})}{\sqrt{\sum(a-\bar{a})^2(b-\bar{b})^2}}, \qquad (11)$$

where a, b are two input variables of the same size, and $\bar{a}$, $\bar{b}$ are the averages of these variables.

The closer correlation coefficient is to 1 or -1, the more linear dependency two variables have. If the correlation coefficient is equal to 0, then there is no linear dependency between them. If the correlation coefficient is higher than 0, then such correlation is called *positive*. If it is lower than 0, then the correlation is called *negative*.

In our research, the correlation between both sets of 2D texture features and 3D roughness parameters was estimated. The correlation between 270 pairs (27 features $\times$ 10 parameters) of vectors was calculated. Every feature and parameter vector has a length of 250 (equal to the amount of the sample images). The distribution of the correlation for all pairs is shown in Figure 5.

For correlation coefficient, an interpretation of the Brosius criteria (Brosius, 1998) was used. These criteria are listed in Table 2. This interpretation of the correlation coefficients gives an easier explanation whether values have a weak or strong correlation.

Table 2: Correlation coefficient interpretation.

Absolute value of coefficient	Interpretation
0	no correlation
$0 < \rho < 0,2$	very weak
$0,2 < \rho < 0,4$	weak
$0,4 < \rho < 0,6$	medium
$0,6 < \rho < 0,8$	strong
$0,8 < \rho < 1$	very strong
1	perfect

5 RESULTS AND DISCUSSION

Previously in the work (Trambitckii et al., 2016) it was mentioned, that a set of texture features, calculated for surfaces with removed waviness, has shown weak correlation with 3D parameters. This phenomenon can be explained. Texture features reflect not only surface roughness, but also a low frequency of the surface – waviness. When the correlation between texture features and roughness parameters is estimated, waviness should not be removed from the 3D surfaces. Thus, in this research raw 3D surface data was used for calculation of roughness parameters.

In this research, the texture features calculated for images of metal surfaces under ring light conditions showed strong (up to 0.8009) correlation between the roughness parameters.

The Pearson's correlation coefficients between 27 texture features and 10 roughness parameters were calculated. It resulted in the array of 270 pair-wise

Table 3: Some correlation coefficients between several pairs.

Roughness parameter	Texture feature	Correlation coefficient
S_a (arithmetical mean height of the surface)	F_{HRA} (histogram range)	0.8009
S_q (root mean square height of the surface)	F_{ICU} (image curvature)	0.7915
S_z (maximum height of the surface)	F_{HEN} (histogram entropy)	0.7826

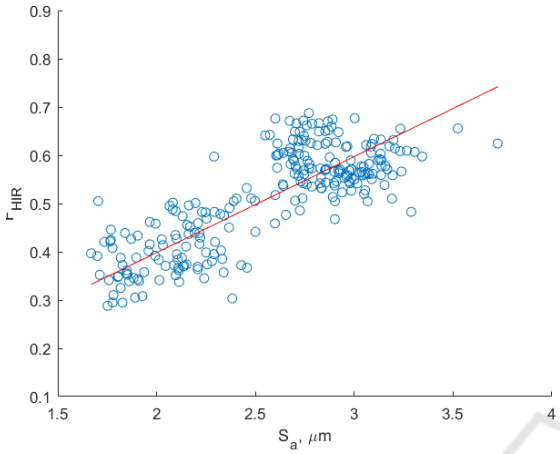

Figure 6: Scatter plot of parameter pairs of the average surface roughness (S_a) and the histogram range (F_{HIR}). Linear regression (*red line*) was performed to get the relationship between these two values. A correlation coefficient between these parameters is equal to 0.8009.

correlation coefficients. For all the coefficients absolute values were calculated, as some of the coefficients have negative values. Then all pairs were sorted from the highest to the lowest values of the correlation coefficients. A plot was created based on this information. The plot shows the distribution of the correlation coefficients for all 270 pairs, see Figure 5. X-axis represents the absolute correlation coefficient value. Y-axis is an index of the pair, sorted by the correlation coefficient value in descending order. 40% of feature/parameter pairs showed a strong ($\rho > 0.6$) correlation. The correlation coefficients of several pairs are listed in Table 3.

The performed research showed that under our conditions the most correlated roughness parameters are S_a, S_q, S_z (see a description of the parameters in Chapter 4.3). The most correlated texture features are the histogram entropy, the histogram range, the image curvature, the steerable filters-based and the spatial frequency (see a description of these features in Chapter 4.2). An example of the most correlated pair (S_a and the histogram range) is shown in Figure 6. An average value of the correlation coefficient between them is equal to 0.8009.

The future work can be focused on the calculation of correlation among different texture features itself. A larger set of parts can be produced to increase the number of images in a dataset. More texture features can be implemented to obtain probably even higher correlation between features and parameters.

The performed research showed that there is a strong correlation between texture features and roughness parameters. This means that texture features can be successfully applied to roughness assessment of metal surfaces, as well as for the estimation of the surface quality. This method of non-contact quality control gives a possibility to find parts with certain defects in a fast and reliable way on the basis of cost-effective hardware equipment. It can help to increase the rate of detection of parts, which are not fulfil given requirements.

6 CONCLUSION

During the research, a set of 27 texture futures was calculated for metal surface images. A set of 10 roughness parameters was calculated for the same metal parts. The correlation between these sets was estimated. 40% of feature/parameter pairs showed a strong ($\rho > 0.6$) correlation. Thus, texture features can reflect roughness information of a surface under the controlled lighting conditions. It shows that texture features can be used to estimate metal surface quality using images obtained with low-cost 2D cameras.

ACKNOWLEDGEMENTS

The research project, which forms the basis of this paper, is supported by the Thuringian Ministry of Economy, Employment and Technology (TMWAT) with means from the European Social Fund (ESF). The responsibility for the content of this paper lies with the author. Special thanks are due to the Society for Production Engineering and Development Schmalkalden (Germany), especially to Dr. Daniel Garten, for providing the measurement equipment and the processed metal parts for the research.

REFERENCES

ISO 25178: Geometric Product Specifications (GPS) Surface texture: areal.

Alegre, E., Alaiz-Rodríguez, R., Barreiro, J., Fidalgo, E., and Fernández, L. (2010). Surface finish control in machining processes using haralick descriptors and neuronal networks. In *Computational Modeling of Objects Represented in Images*, pages 231–241, Berlin, Heidelberg. Springer Berlin Heidelberg.

Benardos, P. and Vosniakos, G.-C. (2003). Predicting surface roughness in machining: a review. 43:833–844.

Brosius, F. (1998). *SPSS 8*. International Thomson Publishing.

C. Gonzalez, R., E. Woods, R., and L. Eddins, S. (2004). *Digital Image Processing Using Matlab*, volume 1.

Chandraratne, M., Samarasinghe, S., Kulasiri, D., and Bickerstaffe, R. (2006). Prediction of lamb tenderness using image surface texture features. 77:492–499.

Chen, Z., Zhang, Z., Shi, J., Chen, R., Huang, R., and Zhang, C. (2008). A multivariate method for surface roughness vision inspection in different ambient light. In *2008 IEEE International Conference on Mechatronics and Automation*, pages 324–328.

Firestone, L., Cook, K., Culp, K., Talsania, N., and Jr., K. P. (1991). Comparison of autofocus methods for automated microscopy.

Geusebroek, J.-M., Cornelissen, F., Smeulders, A. W., and Geerts, H. (2000). Robust autofocusing in microscopy. *Cytometry: The Journal of the International Society for Analytical Cytology*, 39(1):1–9.

Haralick, R. M., Shanmugam, K., and Dinstein, I. (1973). Textural Features for Image Classification. *IEEE Transactions on Systems, Man, and Cybernetics*, SMC-3(6):610–621.

Helmli, F. S. and Scherer, S. (2001). Adaptive shape from focus with an error estimation in light microscopy. In *ISPA 2001. Proceedings of the 2nd International Symposium on Image and Signal Processing and Analysis. In conjunction with 23rd International Conference on Information Technology Interfaces (IEEE Cat.*, pages 188–193.

Krotkov, E. and Martin, J.-P. (1986). Range from focus. In *Robotics and Automation. Proceedings. 1986 IEEE International Conference on*, volume 3, pages 1093–1098. IEEE.

Lee, S.-Y., Yoo, J.-T., Kumar, Y., and Kim, S.-W. (2009). Reduced energy-ratio measure for robust autofocusing in digital camera. *IEEE Signal Processing Letters*, 16(2):133–136.

Liu, L., Zhao, L., Long, Y., Kuang, G., and Fieguth, P. (2012). Extended local binary patterns for texture classification. *Image Vision Comput.*, 30(2):86–99.

Lu, C. (2008). Study on prediction of surface quality in machining process. *Journal of Materials Processing Technology*, 205(1):439 – 450.

M. Eskicioglu, A. and S. Fisher, P. (1996). Image quality measures and their performance. 43:2959 – 2965.

Minhas, R., Mohammed, A. A., Wu, Q. J., and Sid-Ahmed, M. A. (2009a). 3d shape from focus and depth map computation using steerable filters. In *International Conference Image Analysis and Recognition*, pages 573–583. Springer.

Minhas, R., Mohammed, A. A., Wu, Q. M. J., and Sid-Ahmed, M. A. (2009b). 3d shape from focus and depth map computation using steerable filters. In Kamel, M. and Campilho, A., editors, *Image Analysis and Recognition*, pages 573–583, Berlin, Heidelberg. Springer Berlin Heidelberg.

Nanda, H. and Cutler, R. (2001). Practical calibrations for a real-time digital omnidirectional camera. *CVPR Technical Sketch*, 20:2.

Nayar, S. K., Watanabe, M., and Noguchi, M. (1996). Real-time focus range sensor. *IEEE Transactions on Pattern Analysis and Machine Intelligence*, 18(12):1186–1198.

Pech-Pacheco, J. L., Cristóbal, G., Chamorro-Martinez, J., and Fernández-Valdivia, J. (2000). Diatom autofocusing in brightfield microscopy: a comparative study. In *Pattern Recognition, 2000. Proceedings. 15th International Conference on*, volume 3, pages 314–317. IEEE.

Sabino, D. M. U., da Fontoura Costa, L., Gil Rizzatti, E., and Antonio Zago, M. (2004). A texture approach to leukocyte recognition. *Real-Time Imaging*, 10(4):205–216.

Santos, A., Ortiz de Solórzano, C., Vaquero, J. J., Pena, J., Malpica, N., and Del Pozo, F. (1997). Evaluation of autofocus functions in molecular cytogenetic analysis. *Journal of microscopy*, 188(3):264–272.

Shen, C.-H. and Chen, H. H. (2006). Robust focus measure for low-contrast images. In *Consumer Electronics, 2006. ICCE'06. 2006 Digest of Technical Papers. International Conference on*, pages 69–70. IEEE.

Shirvaikar, M. V. (2004). An optimal measure for camera focus and exposure. In *System Theory, 2004. Proceedings of the Thirty-Sixth Southeastern Symposium on*, pages 472–475. IEEE.

Stout, K., Sullivan, P., Dong, W., Mainsah, E., Luo, N., Mathia, T., and Zahouani, H. (1994). *Development of Methods for Characterisation of Roughness in Three Dimensions*. Publication No. EUR 15178 EN of the Commission of the European Communities, Luxembourg.

Subbarao, M., Choi, T.-S., and Nikzad, A. (1992). Focusing techniques. In *Machine Vision Applications, Architectures, and Systems Integration*, volume 1823, pages 163–175. International Society for Optics and Photonics.

Thelen, A., Frey, S., Hirsch, S., and Hering, P. (2009). Improvements in shape-from-focus for holographic reconstructions with regard to focus operators, neighborhood-size, and height value interpolation. *IEEE Transactions on Image Processing*, 18(1):151–157.

Torabi, M., Ardekani, R., and Fatemizadeh, E. (2007). Discrimination between alzheimer's disease and control group in mr-images based on texture analysis using artificial neural network.

Trambitckii, K., Anding, K., Polte, G., and Garten, D. (2014). Elimination of out-of-focus regions for surface analysis in 2-d colour images.

Trambitckii, K., Anding, K., Polte, G., Garten, D., Musalimov, V., and Kuritcyn, P. (2016). The application of texture features to quality control of metal surfaces. *ACTA IMEKO*, 5(4):19–23.

Yang, G. and Nelson, B. J. (2003). Wavelet-based autofocusing and unsupervised segmentation of microscopic images. In *Intelligent Robots and Systems, 2003.(IROS 2003). Proceedings. 2003 IEEE/RSJ International Conference on*, volume 3, pages 2143–2148. IEEE.